PROCEEDINGS OF ECOS 2023 - THE 36TH INTERNATIONAL CONFERENCE ON
EFFICIENCY, COST, OPTIMIZATION, SIMULATION AND ENVIRONMENTAL IMPACT OF ENERGY SYSTEMS
25-30 JUNE, 2023, LAS PALMAS DE GRAN CANARIA, SPAIN

The impact of controller settings in heat pumps: Numerical findings and experimental verification

Stephan Göbel[a], Kevin Waiz[a], Christian Vering[a] and Dirk Müller[a]

[a] RWTH Aachen University, Institute for Energy Efficient Buildings and Indoor Climate, Aachen, Germany, stephan.goebel@eonerc.rwth-aachen.de

Abstract:

In residential buildings, the efficiency of heat pump systems (HPS) significantly depends on the HPS design and operation. In particular, HPS controllers often use ambient temperature-dependent heating curves for operation. The resulting supply temperature serves as the reference variable for the internal controller, which is used to manipulate the compressor speed. Typically, the internal controller has constant parameters for the PI controller, hysteresis, and operational time. While buildings have a highly dynamic, time-variant demand, these dynamics are rarely considered in controller development.

This work investigates internal control parameters' sensitivity to the overall HPS efficiency in annual, dynamic simulations and experiments. To consider different supply temperatures, two buildings with underfloor heating and radiators serve as case studies. Based on a validated simulation model, the one-factor-at-a-time sensitivity analysis method determines the controller's influence on the seasonal coefficient of performance (SCOP). Hardware-in-the-loop experiments are conducted for representative periods extracted from annual simulation results for experimental verification.

The results for the building with underfloor heating and radiators prove that the control parameter influences the SCOP up to 18.5 % and 4.2 %, respectively. In particular, different control parameters for the optimal operation were determined for both case studies, challenging the constant settings used in the state-of-the-art. In addition, we observe a significant increase of 300 % in the avoidable compressor starts in experiments due to poor parameter settings. To ensure maximum efficiency of HPS and significantly reduce the number of compressor starts in any residential building, we recommend integrating adaptive setting of control parameters into the HPS controller.

Keywords:

Sensitivity analysis, hardware-in-the-loop, heating curve, Modelica, inverter-driven, PID, hysteresis.

1. Introduction

Electrically-driven heat pump systems (HPS) are the most efficient solution for the defossilation of the building sector. Since emissions are mainly related to electricity consumption [1], HPS efficiency greatly impacts consumption reduction and thus on emissions.

Besides the refrigerant cycle design which is tailored to operate under dedicated temperature levels (design condition), the HPS controller influences the efficiency in off-design conditions. The controller aims to set the HPS thermal output to the building's heat demand by adjusting the compressor speed. Typically, the control loop begins with a weather compensation heating curve calculating the required supply temperature to reach the heating demand (part I). While On-Off HPS uses a hysteresis controller, inverter-driven HPS also uses a PID controller to realize the link between the set supply temperature and the compressor speed (part II).

Thermodynamic Carnot efficiency strongly depends on the source and supply temperature spread. Aiming for an efficient part I control loop means decreasing the supply temperature as low as possible with a well-designed heating curve or higher control strategies, e.g., model predictive control (MPC). The literature provides different solutions for the part I control loop [2]–[4]. This work focuses on part II of the control loop and uses a heating curve that fits the building load for each case study.

Part II of the control loop translates the set supply temperature value into a compressor speed. This part of the control loop is an internal variable to avoid compressor damage. To the best of the author's knowledge, the literature only provides a few studies about the influence of the part II control loop on the heat pump's efficiency. Uhlmann et al. [5] show in experimental and simulative studies that the loss of efficiency caused by the startup and shutdown processes is less than 2% if a continuous minimum running time of 15 minutes can be ensured. A related study [2] suggests that a compressor running time of at least 20 minutes is required to avoid degradation effects or startup losses. The study shows that the unit control and the system's thermal inertia strongly influence the heat pump's energy losses. Thus, the configuration of the hysteresis control strongly

https://doi.org/10.52202/069564-0075

influences the cycling behavior. Dongellini et al. [6] simulate the dynamic performance of three types of heat pumps (single-stage, multi-stage, and inverter-controlled). The results indicate that the efficiency losses during the heat pump startup process significantly impact the overall system efficiency, especially for single-stage units. In this case, the reduction in SCOP is up to 12%. Xu et al. [7] study focuses on inverter-controlled heat pumps, in particular, the hysteresis parameter of the control. In order to improve the dynamic performance under frequent partial load conditions, a control concept with variable hysteresis of the supply temperature was proposed, in which the lower threshold value increases piecewise with increasing outside air temperature. All the studies mentioned use the manufacturer's inverter control settings, i.e., the PID controller parameters remain unchanged. However, to the best of the author's knowledge, the sensitivity of PID parameters on the efficiency of inverter-controlled heat pumps is not discussed in the literature. Furthermore, the influence of the heat pump's operational behavior is only discussed in the context of efficiency but not on the degradation.

This paper closes the identified research gaps in a simulative and experimental case study:

- To access all parameters of the heat pump's control loop, we conduct measurement campaigns with a fully-controllable heat pump test bench [8].
- To integrate degradation into the evaluation process, we use the number of startups per hour as a key performance indicator (KPI).
- To prove the sensitivity of PID controller parameters, we develop a heat pump controller, which we use in a simulative and experimental case study.
- To verify our simulative results, we use the hardware-in-the-loop approach by coupling a heat pump test bench to a developed heat pump controller and a virtual building.

The paper is divided into five sections:

- Section 2 shows the simulative and experimental setup.
- Section 3 describes the results of the case studies.
- Section 4 discusses the results by underlining the influence of the control loop part II on the efficiency
- Section 5 concludes all findings and gives recommendations for future work.

2. Method

To investigate the sensitivity of the PID controller's parameters and the hysteresis bandwidth to the heat pump process, we develop a simulation model that comprehensively analyzes and evaluates the part II control concept. Subsequently, we use sections of the recorded measurement data in an experimental setup to verify the obtained results on a real heat pump. This section starts with an overview of the simulation models, followed by the experimental setup description, and ends with the introduction of the simulative and experimental case study.

2.1 Building Energy System Simulation

For the adequate execution of a parameter study, we develop a simulation model that computes the conditions of the system in a meaningful way and outputs system variables in a comprehensible and plausible manner. For this purpose, the simulation model of the building energy system (BES), which forms the basis for the parameter study, is presented in Figure 1, including the associated submodels. We develop the BES in Modelica using the Dymola [9] environment. The individual models are generally based on the *BESMod* library [10]. The library draws on *AixLib* [11], *BuildingSystems* [12] and *IBPSA* (basic library of the previous archives) [13].

Figure 1 shows the BES model, which consists of the submodels weather, user, transfer, building, control, generation, and distribution. The latter three together form the sub-model of hydraulics. The weather submodel is based on meteorological data recorded and published by the German Weather Service (DWD) at hourly intervals for a specific region within Germany during a representative year [14]. Concerning an appropriate computational time compared to the effort, we use a reduced building model as a heat sink. We reparametrize the basic model using the TeaserTool [15]. It allows building construction based on information about the net area, number, and height of floors, year of construction, and intended use of the building. The heating load calculated according to EN 12831 is 6596.21 W, and the volume of the heating zone is 325.0 m^3 with a net area of 130.0 m^2.

On the user side, we assume constant behavior to avoid the superposition of effects. For the same reason, we also neglect any internal gains. Therefore, the room's setpoint temperature is constant at 20 °C for each room, regardless of the time of year or day. We consider two systems for the hydraulic heating network within the scope of the analysis. Thermal energy distribution and transfer are accomplished by underfloor heating (UFH) or a radiator. We adopt the models from the *BESMod* library for this purpose. Both models have a throttle and a bypass valve, the latter to decouple the hydraulic cycle and thus protect the system from a sharp rise in the heating water pressure.

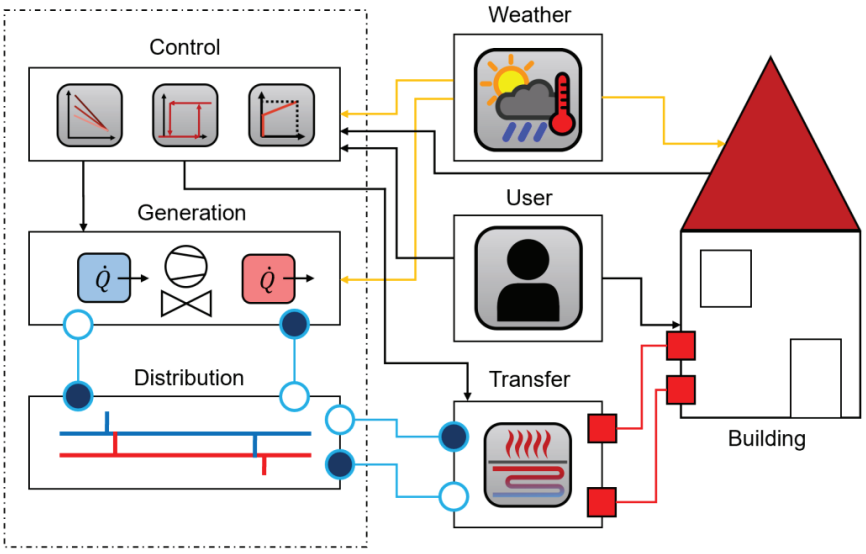

Figure 1: Simulation structure of the building energy system - With fluid flows in blue, heat flows in red, weather data in yellow and data transfer in black as connecting elements [10].

We have mapped the adapted control of the system in the *MonovalentOptihorst* model. In addition to the hysteresis-based heating curve controller, it also contains the integration of safety functions. With the help of the room temperature set by the user $T_{set,Room}$, and the current outdoor temperature T_{amb}, the heating curve specifies the required supply temperature T_{set}. The downstream hysteresis controller uses the difference between T_{set} and T_{sup} and determines whether the heat pump sets its operating mode to On or Off. If the supply temperature exceeds the set temperature by half of the set bandwidth of the hysteresis, the heat pump is switched off until it reaches the lower limit (T_{set} - $Hys/2$). This on/off-signal and T_{set} are then used via the PI controller to set the compressor speed n_{set} is output. The *SecurityControl* [16] model of *AixLib* then checks compliance with the safety functions and operating limits. In addition to the minimum runtime and resting time, these also include the maximum number of start operations per hour. Triggering the safety functions causes the heat pump to shut down or to continue running, depending on which safety function takes effect. For example, compliance with the minimum running time requires the machine to continue running to prevent damage, even though a signal from the PI control wants to switch it off.

The simulation model of the heat pump corresponds to the *HeatPumpAndHeatingRod* model of *BESMod*. We use a black-box model, which specifies the required electrical power P_{el} and the resulting heating power $\dot{Q}_{\text{Con}}$ as a function of the supply temperature, the inlet temperature of the evaporator, and the compressor speed. When the compressor is switched on, it immediately requires electrical power. The problem of the missing dynamics of the model in relation to the provision of the heat is mitigated by the interposition of a PT3 element. Through the PT3 element, we can implement an artificial inertia, resulting in a delay of the effective heat flow analogously to the real system. The duration of the delay can be determined by the setting of a constant parameter, which corresponds to a cut-off frequency. [16]

To integrate the established model's dynamic processes within the heat exchangers and the mentioned cut-off frequency, we conduct experimental tests on a real heat pump to calibrate the model with the measured data. We calibrate the adjusted heat pump model using the fully-controllable heat pump test bench, which is also used in the experimental case study. Basically, calibration refers to the variation of model parameters so that the difference between simulated and measured values is as small as possible. Therefore, we use parameters of the condenser, such as the heat transfer coefficients or the condenser volume, and the cut-off frequency to match simulated and measured values. The program AixCaliBuHA [17] is used to calibrate the system. It allows the automatic calibration of dynamic buildings and heating systems using the Python-Dymola interface.

The different operating conditions associated with the inverter technology, as a result of the variably adjustable compressor speed, necessitate the inclusion of dynamic factors in the calibration. For example, several different temperatures are set for the source and sink in succession during the temperatures are set for the source and sink to compensate for the resulting transient and departure processes. For the calibration process, we record the temperatures T_{amb}, T_{sup} and T_{ret}, the mass flow in the condenser, the electrical power of the compressor P_{el} as well as the speed of the compressor. Here, P_{el} and T_{sup} correspond to the target variables of the calibration. The four remaining quantities are used as real input for the simulation. The temporal

https://doi.org/10.52202/069564-0075

resolution of the data intervals is one second, and the period of consideration is 8800 s. As a basis for evaluation, we use a normalized weighted error measure (NRMSE), which gives equal and scale-independent weight to both target variables.

The corresponding curves of the simulated and measured quantities for the minimum NRMSE are visualized in Figure 2. It can be seen that especially the supply temperature is sufficiently modeled. Quantitatively, this can also be confirmed with an NRMSE of less than one percent. The higher NRMSE for the electrical power of 2.37% is due to inaccuracies between 8000 - 8800 s. The noticeably broader curve section of the magnitude in this interval can be derived from perceived speed oscillations while recording the experimental measurement data. Overall, we achieve a final NRMSE of 1.658%. This can be considered a positive result; other works obtained results in a comparable range [16], [18].

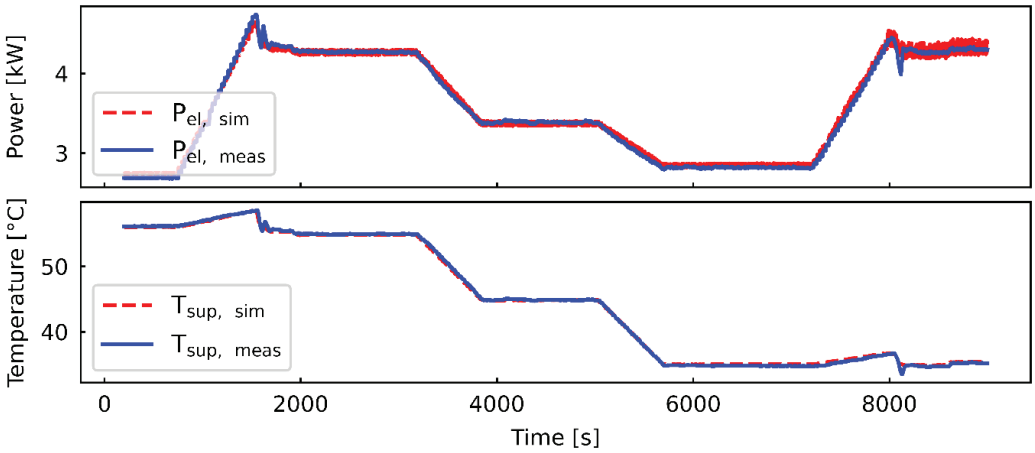

Figure 2: Visualization of the measured target variables $P_{el,meas}$, $T_{sup,meas}$ and the corresponding simulation variables $P_{el,sim}$, $T_{sup,sim}$.

2.2 Experimental setup

We validate all our findings in this work with experiments using the hardware-in-the-loop (HiL) approach and a fully-controllable heat pump test bench. The HiL approach connects virtual buildings to the heat pump by emulating the weather conditions and the thermal heat flows. Figure 3 shows the schematic overview of the experimental setup. The system consists of an air-to-water heat pump test bench in split design, which is fully controllable, test benches emulating the boundary conditions (climatic chamber and hydraulic test bench), simulation models for the building and the heat pump controller, and the cloud-based data infrastructure (MQTT-Broker and InfluxDB tick-stack). The used HiL approach and the corresponding test benches are well described in the literature [19], [20]. In this study, we use a self-developed heat pump test bench where we can freely control the compressor speed. The heat pump test bench has its own PLC, which gets the current set compressor speed via MQTT. Only necessary safety controllers (e.g., superheat) are part of the heat pump test bench. Further details about the test bench and its internal control can be found in the literature [8].

With the help of our method, it is possible to change between a pure simulation model and a HiL experiment without significant effort. Only the submodels of heat generation and distribution are swapped to communication models. Measured values (e.g., supply temperature) are subscribed from the test bench, and relevant values for the heat pump (e.g., return temperature) are published to the test bench.

We develop and calibrate our building energy system simulation models with the experimental setup to perform verified annual simulations and experimental results.

2.3 Annual and daily simulative case study

We use the one-factor-at-a-time (OFAT) method [21] for the annual and daily horizons parameter study. Here a single parameter is varied while the remaining ones assume constant reference values. The advantage of the OFAT method is that overlaps and synergies can be excluded by varying a single parameter. Thus we can relate system changes to modifying the input variable.

In the preliminary state of the parameter study, the framework conditions of the analysis must be defined. Table 1 shows the value ranges of the control parameters, the reference values, the safety functions' values, and the other models' relevant values. The control parameters consist of the proportionality factor K_P, the integral time T_N and the hysteresis bandwidth *Hys*. In the annual simulation studies, the proportionality factor K_P and the integral time T_N varies from 0.00001 to 20 and from 10 s to 50000 s, respectively, on a logarithmic

scale. We set the corresponding reference values to 0.5 and to 1000 s. Performing the OFAT method with the chosen parameter variation results in 42 simulations for each system. Thus, we perform a total of 82 annual simulations.

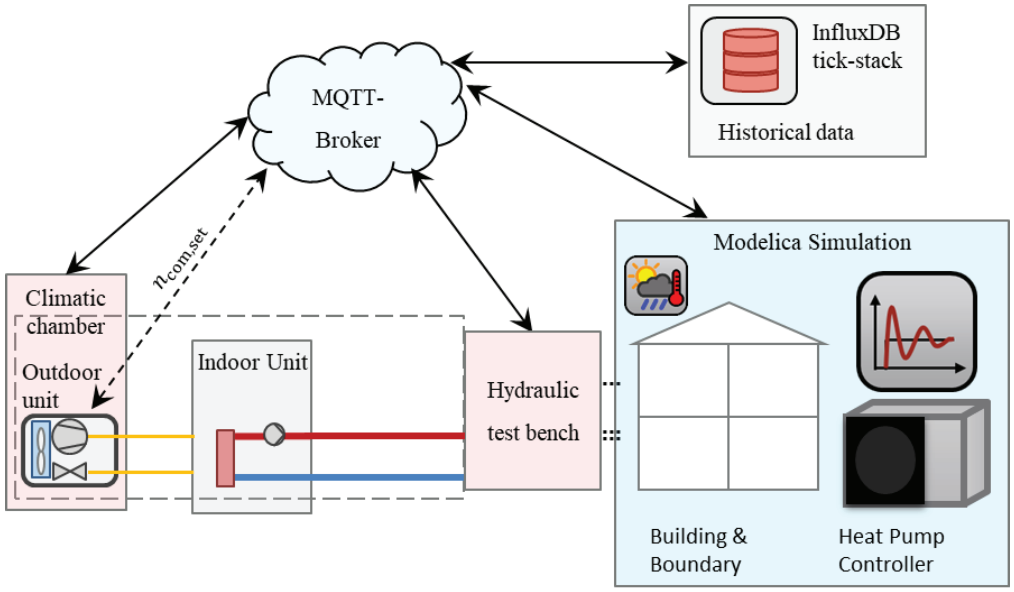

Figure 3: Schematic overview of HiL setup: heat pump test bench (indoor unit and outdoor unit), climatic chamber, hydraulic test bench, simulation model, InfluxDB tick-stack, and MQTT Broker

The safety parameters allow the heat pump to run a maximum of 10 times per hour for a minimum running time of 180 s. The resting time after shutdown has to be a minimum of 180 s. In addition, the maximum supply temperature is set to 70 °C. The presented simulation model with the underfloor system has a nominal supply temperature of 40 °C and a nominal mass flow of 0.315 kg/s. The system with radiators uses a nominal supply temperature of 55 °C with a nominal mass flow of 0.197 kg/s.

A detailed look into the operation behavior is realized with representative days. Thus, the interaction of the outdoor temperature and the solar irradiation with the variation of the control parameters can be considered in a bundled way. The outdoor temperatures of the three used representative days can be seen in Figure 4. The days correspond to representative periods calculated using the k-medoids clustering [22] and cover three different temperature levels.

Table 1: Value ranges, step sizes, and reference values of the controlled variables, the safety functions, and operating variables of both transfer systems.

Control parameter	Min. value	Max. value	Step size	Reference value
Proportionality factor K_p	0.00001	20	Log	0.5
Integral time T_N	10 s	50000 s	Log	1000 s
Hysteresis bandwidth	1 K	12 K	1 K	8 K

Safety parameter	Value	Transfer parameter	Value
Max. runs per hour	10	UFH - nominal supply temperature	40 °C
Min. run time	180 s	UFH – mass flow	0.315 kg/s
Min. rest time	180 s	Rad. - nominal supply temperature	55 °C
Max. supply temperature	70 °C	Rad. – mass flow	0.197 kg/s

2.4 Experimental case study

Test runs under real conditions are necessary to validate the results obtained. Since field tests in real buildings are costly and time-consuming, we perform HiL experiments to emulate almost field behavior.

We conduct three experiments for the underfloor and radiator system. We vary the hysteresis bandwidth for each system from a low level over the reference level to a high level. The goal of the experiments is to validate the method and underline that the developed controller leads to the same operation behavior for the simulation model and the heat pump test bench.

https://doi.org/10.52202/069564-0075

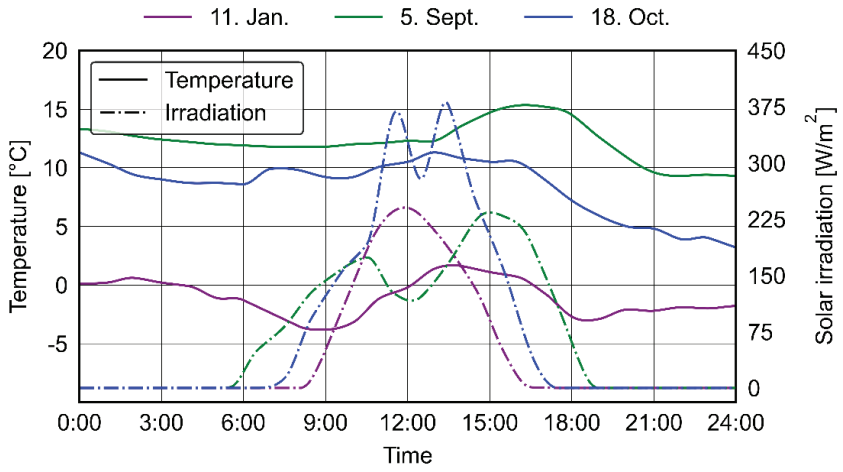

Figure 4: Outdoor temperature and solar irradiation for the reference days in Potsdam in 2015.

3. Results

This section starts with the sensitivity analysis results, which are mainly simulative performed and ends with the validation with the help of experimental results.

3.1 Simulative case study: sensitivity analysis

In order to visualize the effect of control parameters, it can be seen from Figure 5 to what extent different parameter values influence the number of daily on/off cycles. As shown in Figure 5 (a) for using a UFH, the number of cycles for a hysteresis bandwidth of 2 K below a temperature of 10 °C is increased in contrast to the use of a bandwidth of 10 K. Thereby, the number of cycles for a bandwidth of 2 K often reaches its maximum of 240 cycles per day. Notably, for a bandwidth of 10 K, the number of cycles initially increases at -5 °C before decreasing again from a temperature of 10 °C. A similar picture is also provided using K_p= 0.00001, shown in Figure 5 (b). Again, the daily cycles decrease for temperatures above 10 °C. Analogous to UFH, the radiator increases cycles for a decreased bandwidth. According to Figure 5 (c), we can identify a trend for the use of a bandwidth of 2 K and 10 K, according to which the number of cycles decreases with a rising outdoor temperature and the number of cycles increases with smaller hysteresis. Only using low proportionality factors ensures that the cycles decrease for outdoor temperatures below 5 °C, so the scatter plots of UFH and radiator show comparable results.

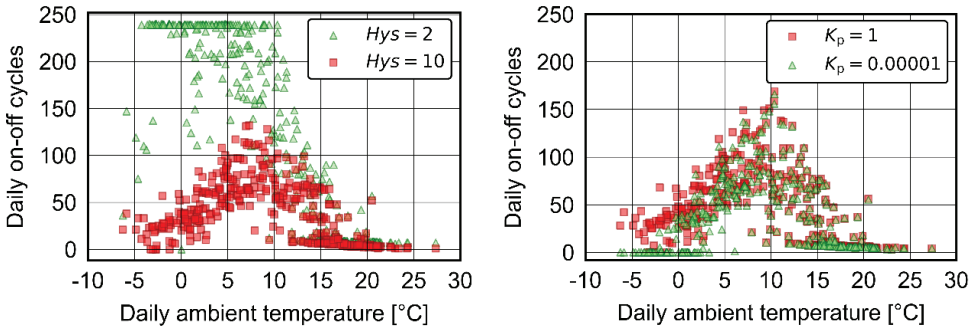

(a) UFH – Hysteresis

(b) UFH – Proportionality factor

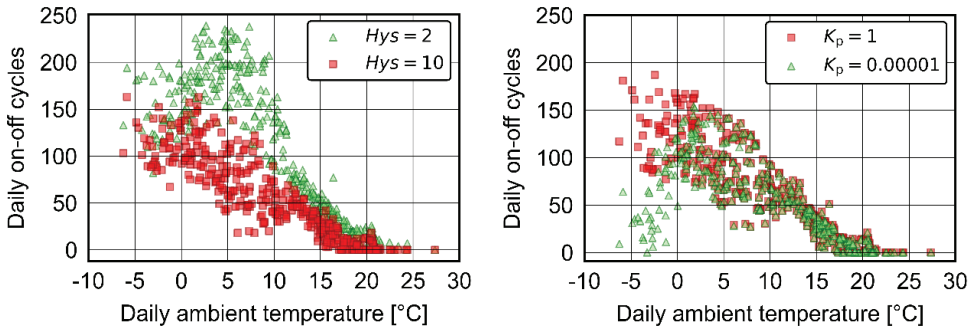

(c) Radiator – Hysteresis (d) Radiator – Proportionality factor

Figure 5: Representation of the annual simulation's daily on/off cycles when using UFH (a,b) or radiator (c,d) as a function of the ambient temperature.

Figure 6 (a,c) shows that the Kp and TN boundary values represent the SCOP's respective minima and maxima. The variation's optimum reset time is at T_N = 50,000, with a value of 3.2. Whereas an increase of K_p continuously decreases the system efficiency, we observe an efficiency drop for T_N = 50 - 150. The SCOP decreases to a value of up to 2.70, corresponding to a relative change concerning the maximum efficiency of 15.6 %. We detect that the efficiency initially increases with a rising hysteresis bandwidth before continuously decreasing from a value of three Kelvin (Figure 6 (e)). Here, a SCOP maximum of 3.25 (3 K) contrasts with a minimum of 3.14 (12 K). The relative change is 3.6 %.

For the radiator as a heat sink, analogous to using UFH, we notice that the boundary values for K_p and T_N represent the maxima and minima. Again, K_p = 0.00001 and T_N = 50,000 s correspond to the highest SCOP parameters (cf. Figure 6 (b,d)). Their use implies a SCOP of 2.60 and 2.58, with the resulting relative efficiency differences of 3% and 3.9%, respectively. For the integral time variation, a noticeable reduction of the SCOP to 2.48 is shown only for T_N = 10.

For the proportionality factor, we observe that its increase means an increase in the cycles by up to 25 %. The hysteresis bandwidth's variation yields a maximum SCOP of 2.58 for a bandwidth of 12 K. Despite an increasing number of cycles with decreasing bandwidth, we cannot detect a significant change in efficiency (cf. Figure 6 (f)). The number of cycles increases by almost 250 %, while the SCOP varies only within a range of 2 %.

An overview of the obtained results of the most efficient parameter values for the considered periods is given in Table 2. It contains the SCOP, the relative change of the SCOP from the minimum to the maximum value (ΔSCOP), and the number of cycles per control variable and period. The associated results for the variation of the proportionality factor for both transfer systems show that the maximum values are different not only for the representative days but also for the same day for different transfer systems. Except for a proportionality factor of 0.00001 for the annual simulation, none of the best values for a given reference day are the same. For example, a value of 0.0001 for the UFH is compared to 0.1 for the radiator on 10/18. We recognize that the number of cycles increases with the average day temperature for the UFH system. At the same time, the SCOP rises with an increasing temperature for both transfer systems to a maximum of 3.77 and 3.02, respectively.

It is noticeable that proportionality between the number of cycles and the efficiency can only be determined to a limited extent. For the variation of K_p and T_N when using a radiator, the increasing number of cycles from reference day 01/11 to 10/18 inevitably increases efficiency due to the higher temperature level. However, comparing the various results of the control variables for a given day shows that more cycles do not necessarily result in lower efficiency. For example, we observe that for the under-floor heating on 10/18, the SCOP maximum of the hysteresis with a value of 3.51 at 156 cycles is higher than the respective maximums of the other two control variables, although their cycle numbers are lower (107).

Considering the ΔSCOP according to Table 2, we notice that the variation of T_N causes a high deviation, equivalent to a high sensitivity. Thus, we observe a deviation of 46.3 % for reference day 01/11 when UFH is used. The hysteresis variation also shows a high value of 27.3 % compared to the deviation of the remaining variables.

The collected consideration of the results finally show that the integral time T_N has the most significant sensitivity overall. As a variation result, it causes a deviation of 18.5 % (UFH) and 4.2 % (Radiator) from the lowest to the highest SCOP within the annual simulation and also shows the largest percentage on average for the reference days. Only when the radiator is used the hysteresis causes a significantly higher sensitivity

https://doi.org/10.52202/069564-0075

of 18.2 % and 11.0 %, respectively, for reference days 10/18 and 05/09. The various proportionality factors result in a deviation for the UFH and the radiator of 7.4 % and 3.2 %, respectively. Hysteresis has the lowest influence in annual simulation, with a difference of 3.2 % and 1.7 %, respectively.

Table 2: SCOP, relative change of SCOP from minimum to maximum value (ΔSCOP) and absolute number of cycles for a parameter variation of Kp ,TN and the hysteresis bandwidth for reference days and an annual simulation (AS). Listed are the highest values determined based on SCOP.

Reference days/ Annual simulation	Underfloor heating				Radiator			
	11.01	18.10	05.09	AS	11.01	18.10	05.09	AS
K_p - Value	**0.00001**	**0.0001**	**0.05**	**0.00001**	**0.01**	**0.1**	**0.75**	**0.00001**
SCOP	3.14	3.44	3.77	3.32	2.27	2.95	3.02	2.60
ΔSCOP / %	8.40	7.10	5.00	7.40	9.10	5.40	5.60	3.20
Cycles per day	25	107	130	39	113	120	63	57
T_N - Value	**50000**	**35000**	**1500**	**50000**	**50000**	**20000**	**100**	**50000**
SCOP	3.00	3.44	3.78	3.30	2.26	2.95	3.03	2.58
ΔSCOP / %	46.30	14.30	8.10	18.50	9.70	8.40	8.60	4.20
Cycles per day	25	107	130	41.77	113	120	63	59.26
Hysteresis bandwidth	**5 K**	**4 K**	**9 K**	**3 K**	**12 K**	**12 K**	**11 K**	**12 K**
SCOP	2.93	3.51	3.80	3.25	2.24	3.05	3.12	2.59
ΔSCOP / %	27.30	4.50	5.80	3.20	3.20	18.20	11.00	1.70
Cycles per day	38	156	121	122.93	126	78	54	49.98

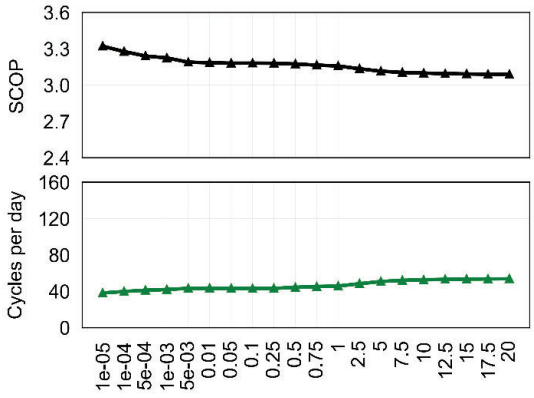

(a) UFH – Proportionality factor K_p [-]

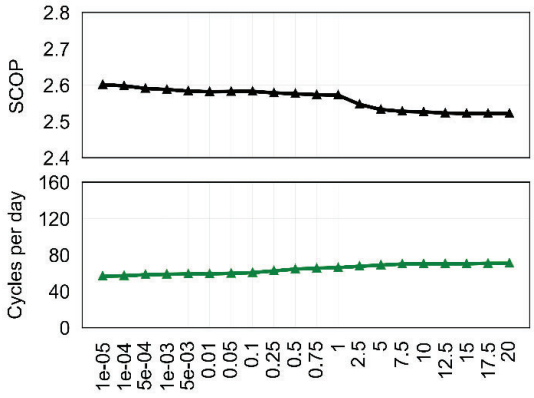

(b) Radiator – Proportionality factor K_p [-]

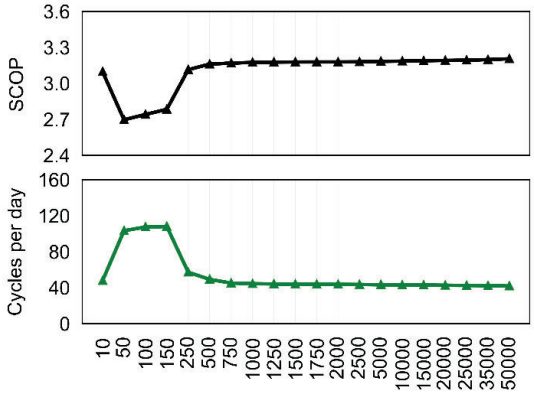

(c) UFH – Integral time T_N $[s]$

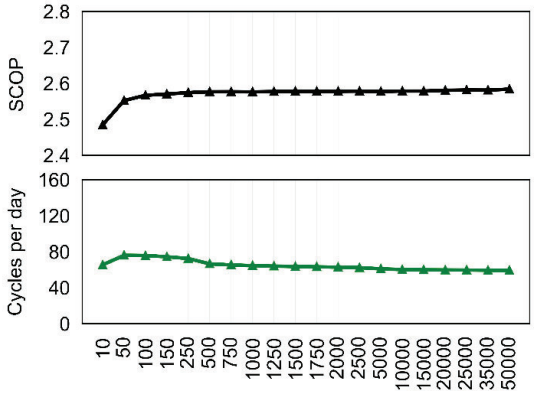

(d) Radiator – Integral time T_N $[s]$

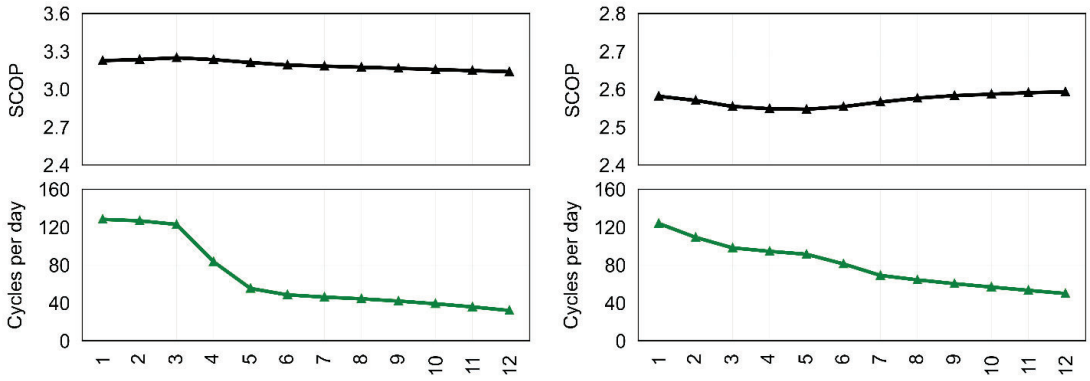

(e) UFH – Hysteresis (f) Radiator – Hysteresis

Figure 6: Comparison of the SCOP and the cycles per day for the annual simulation with different parameter values for the UFH (left) and the radiator (right).

3.2 Experimental case study: validation experiments

The conducted experiments underline the essential findings and trends. First, the developed controller results in equal operation behavior. Figure 7 compares the heat pump's supply and return temperature between the simulation (red) and the experiment (blue). The one-hour experiment begins with the start of the heat pump. After approximately 20 minutes, the experiment and the simulation resulted in similar behavior. The negligible error of under 0.2 K between simulation and experiments underlines the accurate simulation model and validates its application.

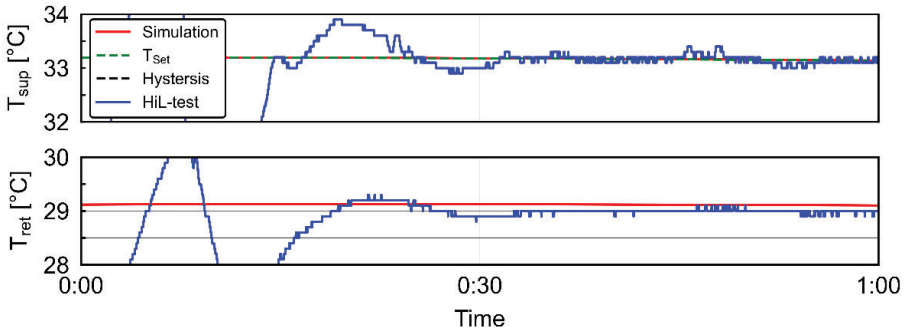

Figure 7: Comparison of supply temperature T_{sup}, and return temperature T_{ret} of the UFH system between simulation (red) and experiment (blue) for $Hys = 8\,\mathrm{K}$ on reference day 01/11.

Nevertheless, we also observe differences between simulation and experiment. Figure 8 compares supply and return temperatures between the simulation (red) and the experiment for the same day but with a lower hysteresis bandwidth of 2 K. The experiment the general operation behavior with many startups within one hour but at different temperature levels. The differences arise from an inaccurate mapping of the model's startup process and additional inertias on the test stand, such as leads, that were not part of the calibration process. In general, the successfully performed experiments show the applicability of the method and the possibility of fast model validation.

https://doi.org/10.52202/069564-0075

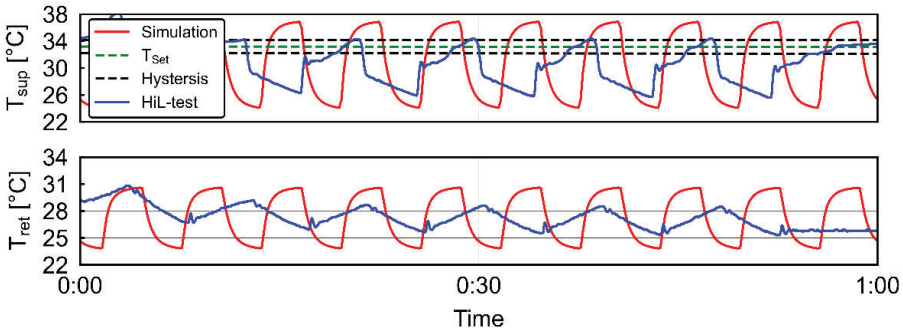

Figure 8: Comparison of supply temperature T_{sup}, and return temperature T_{ret} of the UFH system between simulation (red) and experiment (blue) for $Hys = 2\ \mathrm{K}$ on reference day 01/11

4. Discussion

The following section discusses the obtained results in the context of the literature and is divided into four sections. While many studies discuss the heat pump's operation behavior only in the context of efficiency, we suggest considering the influence on the heat pump's service life (1). Furthermore, we observed discrete operating changes during periods with high solar irradiation (2) and due to bad hysteresis parametrization (3). Control parameters are also sensitive to the transfer system and boundary condition (4).

Typically, in the literature, system operation is only discussed concerning efficiency. Nevertheless, in this context, attention must be paid to assessing the system's service life due to the increased compressor starts. The service life is influenced by the number of operating hours and the frequency of the starting processes. For example, Perrin [22] found that a 12% increase in cycles can reduce compressor life by up to 15%. Therefore, overall consideration of the cycles is imperative for a comprehensive analysis.

The interplay between transfer mass flow and solar irradiation significantly influences the cyclic behavior of the system. From the analysis of the daily simulations, we found that for both transfer systems, there are significant amplitudes of the supply temperature in the midday hours compared to the morning and evening hours. The reason for this is the lack of a buffer tank, which significantly changes the inertia of the sink and solar irradiation. Lower heat output is required when solar irradiation heats the building midday. However, the heating curve only depends on the outdoor temperature, and the solar irradiance is not considered to determine the reference variable T_{set}. The result is that the overflow valve trips as a result of the rising pressure, thus reducing the transfer mass flow to a minimum. This causes high amplitudes of the supply temperature due to that low mass flow. Such cycles result in the system overshooting continuously due to the high control deviation. Because the cooling process is delayed due to the high amplitudes, fewer cycles can be observed overall if this operating state continues for longer. A cycles comparison of the radiator with the aid of Table 2 shows that this issue explains that the number of cycles is almost halved from reference day 10/18 to day 09/05. Accordingly, solar irradiation can result in a tipping point from which the heat pump operating switches from continuous to cycling behavior.

The interaction of the control variables, particularly the hysteresis, with the starting process, can also be regarded as a tipping point which we observe in the validation experiments using the real heat pump. For example, a hysteresis bandwidth of 6 K results in cyclic behavior, while a hysteresis bandwidth of 8 K results in continuous operation. Here, the startup process leads to a supply temperature that slightly exceeds the hysteresis's upper limit and thus maintains the cyclic state. Accordingly, there are threshold values which, as a result of the compressor starting process, mean different characteristics of the operation if they are under or exceeded. However, these threshold values differ between simulation and experiment since the starting process is not accurately modeled.

From the findings of Section 3 and Table 2, we can conclude that both the parameters by themselves in their variation influence the efficiency, and also, the transfer systems show different deviations concerning a SCOP maximum for the same day. Therefore, it is possible to adjust the controller to the building to increase efficiency. Furthermore, since differences in the SCOP-maximum parameter values for the different representative days can be found, the control should be adapted to the ambient conditions. One option for this is the adaptation of the control variables depending on the season or, ideally, based on weather forecasts for the following days.

Conclusion

This work contributes to the defossilation of the building sector by indicating the sensitivity of HPS controller settings on the efficiency and the service life of heat pump systems. In this paper, we develop a simulation model for Building Energy Systems applicable to purely simulation studies and hardware-in-the-loop experiments. The performed sensitivity analysis is based on 82 annual simulations considering various parameters for the proportional factor, the integral time, and the hysteresis bandwidth. We validate the trend of the annual results in further measurement campaigns with a fully-controllable heat pump test bench. The results show the impact of the controller settings on the heat pump's efficiency and operating behavior. Therefore, we analyze the daily heat pump's startups besides the SCOP. We show that the controller parameters influence the SCOP up to 18.5 %, and bad settings can increase the number of compressor starts up to 300 %. Furthermore, the results show discrete steps and nonlinear efficiency values over various parameters, which results from tipping points from which the heat pump operating switches from continuous to cycling behavior.

We will integrate the heat pump's starting process into the simulation model to increase the model's accuracy in future work. Further controller comparisons with the help of the experimental setup will support the efficient development of future systems. Dedicated studies should analyze the influence of the transfer system in more detail by focusing on the system's inertia.

Acknowledgments

We gratefully acknowledge the financial support by the German Federal Ministry for Economic Affairs and Climate Action (BMWK), promotional reference 03EN1022B and 03ET1595A.

not in the reviewed version

Nomenclature

Acronym

BES	building energy system
HIL	Hardware-in-the-loop
HPS	heat pump system
KPI	key performance indicator
MPC	model predictive control
OFAT	one-factor-at-a-time
UFH	underfloor heating

Variables:

Hys	hysteresis bandwidth, K
K_p	proportionality factor
$\dot{m}$	mass flow rate, kg/s
n	rotational speed, 1/s
P	power, W
$SCOP$	seasonal coefficient of performance
T	temperature, °C/K
T_n	integral time

Greek symbols

η	efficiency
φ	maintenance factor

Subscripts and superscripts

amb	ambient
el	electric
ret	return
sup	supply

https://doi.org/10.52202/069564-0075

References

[1] C. Vering, D. Schwarz, P. Stefaniak, V. Venzik, and D. Müller, ‘Kältemittel in Wärmepumpen für die Gebäudeheizung: Ökologische Auswirkungen im gesamten Lebenszyklus’, *Chemie Ingenieur Technik*, vol. 94, no. 4, pp. 542–554, Apr. 2022, doi: 10.1002/cite.202100016.

[2] P. Stoffel, L. Maier, A. Kümpel, T. Schreiber, and D. Müller, ‘Evaluation of Advanced Control Strategies for Building Energy Systems’, Social Science Research Network, Rochester, NY, SSRN Scholarly Paper 4251878, Oct. 2022. Accessed: Oct. 23, 2022. [Online]. Available: https://papers.ssrn.com/abstract=4251878

[3] S. Göbel, C. Vering, and D. Müller, 'Experimental Investigation of Rule-Based Control Strategies for Hybrid Heat Pump Systems Using the Smart Grid Ready Interface', in *PROCEEDINGS OF ECOS 2022*, Kopenhagen, 2022.

[4] J. Drgoňa *et al.*, 'All you need to know about model predictive control for buildings', *Annual Reviews in Control*, Sep. 2020, doi: 10.1016/j.arcontrol.2020.09.001.

[5] M. Uhlmann and S. S. Bertsch, 'Theoretical and experimental investigation of startup and shutdown behavior of residential heat pumps', *International Journal of Refrigeration*, vol. 35, no. 8, pp. 2138–2149, Dec. 2012, doi: 10.1016/j.ijrefrig.2012.08.008.

[6] M. Dongellini and G. L. Morini, 'On-off cycling losses of reversible air-to-water heat pump systems as a function of the unit power modulation capacity', *Energy Conversion and Management*, vol. 196, pp. 966–978, 2019, doi: 10.1016/j.enconman.2019.06.022.

[7] Z. Xu *et al.*, 'Field experimental investigation on partial-load dynamic performance with variable hysteresis control of air-to-water heat pump (AWHP) system', *Applied Thermal Engineering*, vol. 182, p. 116072, 2021, doi: 10.1016/j. applthermaleng.2020.116072.

[8] S. Göbel, T. Fiedler, J. Klingebiel, C. Vering, and D. Müller, 'Development and experimental validation of model-based superheat control strategies for air-to-water heat pumps.' International Institute of Refrigeration (IIR). doi: 10.18462/IIR.GL2022.0143.

[9] Dymola, 'Dymola - Dynamic Modeling Laboratory Full User Manual', 2021.

[10] F. Wüllhorst, L. Maier, D. Jansen, L. Kühn, and Hering, D., and Müller, D., ‘BESMOD – A Modelica Library for Providing Building Energy System Modules’, *THE AMERICAN MODELICA 2022 CONFERENCE*, vol. 2022, pp. 9–19, 2022, doi: 10.3384/ECP211869.

[11] EBC, *AixLib: A Modelica model library for building performance simulations*. 2018. [Online]. Available: https://github.com/RWTH-EBC/AixLib

[12] C. Nytsch-Geusen, J. Huber, M. Ljubijankic, and J. Rädler, ‘Modelica BuildingSystems − eine Modellbibliothek zur Simulation komplexer energietechnischer Gebäudesysteme’, *Bauphysik*, vol. 35, no. 1, Art. no. 1, Feb. 2013, doi: 10.1002/bapi.201310045.

[13] International Building Performance Simulation Association (IBPSA), 'Modelica IBPSA Library'. https://github.com/ibpsa/modelica-ibpsa

[14] D. Wetterdienst, ‘Deutscher Wetterdinest’, 2021. [Online]. Available: https://www.dwd.de/DE/Home/home_node.html

[15] P. Remmen, M. Lauster, M. Mans, M. Fuchs, T. Osterhage, and D. Müller, 'TEASER: an open tool for urban energy modelling of building stocks', *Journal of Building Performance Simulation*, vol. 11, no. 1, Art. no. 1, Jan. 2018, doi: 10.1080/19401493.2017.1283539.

[16] F. Wüllhorst, ‘Implementierung eines Grey-Box-Wärmepumpenmodells in Modelica mit Fokus auf sicherheitsrelevante Regeleinrichtungen’, Bachelorarbeit, 2018.

[17] F. Wüllhorst, T. Storek, P. Mehrfeld, and D. Müller, 'AixCaliBuHA: Automated calibration of building and HVAC systems', *Journal of Open Source Software*, vol. 7, no. 72, p. 3861, 2022, doi: 10.21105/joss.03861.

[18] M. Steinbach, ‘Erstellung und Analyse energetischer Gebäudesimulationen mit Fokus auf kalibrierte Modelle von hybriden Wärmepumpensystemen’. RWTH Aachen University, E.ON Energy Research Center, Institute for Energy Efficient Buildings and Indoor Climate, Jul. 2018.

[19] M. J. Nürenberg, P. Mehrfeld, K. Huchtemann, and D. Müller, 'Hardware-in-the-Loop test bench setup and its application to determine seasonal performance of heat pump systems', 12th IEA Heat Pump Conference 2017, Rotterdam (Netherlands), 15 May 2017 - 18 May 2017, 2017. [Online]. Available: http://publications.rwth-aachen.de/record/712437

[20] P. Mehrfeld *et al.*, 'Dynamic evaluations of heat pump and micro combined heat and power systems using the hardware-in-the-loop approach', *Journal of Building Engineering*, vol. 28, p. 101032, Mar. 2020, doi: 10.1016/j.jobe.2019.101032.

[21] V. Czitrom, 'One-Factor-at-a-Time versus Designed Experiments', *The American Statistician*, vol. 53, no. 2, p. 126, 1999, doi: 10.2307/2685731.

[22] K. Huchtemann, H. Engel, P. Mehrfeld, M. Nürenberg, and D. Müller, 'Testing method for evaluation of a realistic seasonal performance ofheat pump heating systems: Determination of typical days', in *CLIMA 2016 - proceedings of the 12th REHVA World Congress // CLIMA 2016*, P. K. Heiselberg, Ed., [Aalborg: University, 2016.